Title: The master developmental regulator Jab1/Cops5/Csn5 is essential for proper bone growth and survival in mice

Authors: William E. Samsa[1,2], Murali K. Mamidi[1,2], Bryan S. Hausman[1], Lindsay A. Bashur[1], Edward M. Greenfield[4], and Guang Zhou[1,2,3]

Affiliations: Case Western Reserve University, Cleveland, OH, 44106, USA [1]Department of Orthopaedics, [2]Case Comprehensive Cancer Center, [3]Department of Genetics and Genome Sciences, [4]Indiana University School of Medicine, Indianapolis, IN, 46202.

Running Title: Jab1 in osteoblast precursors

Keywords: Jab1/Csn5/Cops5; COP9 Signalosome; Osteoblast Precursors; TGFβ/BMP Signaling; Bone Microarchitecture

Financial Support: NIAMS R01 AR068361, to G.Z., NIDCR R03 DE019190 and DE019190A1S1 to G.Z., NIAMS T32 AR7505-30 to W.E.S. and L.A.B.,

Corresponding Author: Guang Zhou, Ph.D., Case Western Reserve University, Department of Orthopaedics, Biomedical Research Building, #328, 2109 Adelbert Rd, Cleveland, OH, 44106, (216) 368-2260, gxz27@case.edu

Conflicts of Interest: The authors declare no potential conflicts of interest.

Others: Word count: 5673

This is the author's manuscript of the article published in final edited form as:

Samsa, W. E., Mamidi, M. K., Hausman, B. S., Bashur, L. A., Greenfield, E. M., & Zhou, G. (2021). The master developmental regulator Jab1/Cops5/Csn5 is essential for proper bone growth and survival in mice. Bone, 143, 115733. https://doi.org/10.1016/j.bone.2020.115733

ABSTRACT

Jab1, also known as Csn5/Cops5, is a key subunit of the COP9 Signalosome, a highly conserved macromolecular complex. We previously reported that the conditional knockout of *Jab1* in mouse limb buds and chondrocytes results in severely shortened limbs and neonatal lethal chondrodysplasia, respectively. In this study, we further investigated the specific role of *Jab1* in osteoblast differentiation and postnatal bone growth by characterizing a novel mouse model, the *Osx-cre; Jab1*$^{flox/flox}$ conditional knockout (*Jab1 cKO*) mouse, in which *Jab1* is deleted in osteoblast precursor cells. *Jab1 cKO* mutant mice appeared normal at birth, but developed progressive dwarfism. Inevitably, all mutant mice died prior to weaning age. The histological and micro-computed tomography analysis of mutant long bones revealed severely altered bone microarchitecture, with a significant reduction in trabecular thickness. Moreover, *Jab1 cKO* mouse tibiae had a drastic decrease in mineralization near the epiphyseal growth plates, and *Jab1 cKO* mice also developed spontaneous fractures near the tibiofibular junction. Additionally, our cell culture studies demonstrated that *Jab1* deletion in osteoblast precursors led to decreased mineralization and a reduced response to TGFβ and BMP signaling. Moreover, an unbiased reporter screen also identified decreased TGFβ activity in *Jab1*-knockdown osteoblasts. Thus, Jab1 is necessary for proper osteoblast differentiation and postnatal bone growth, likely in part through its positive regulation of the TGFβ and BMP signaling pathways in osteoblast progenitor cells.

Keywords: Jab1/Csn5/Cops5; COP9 Signalosome; Osteoblast Precursors; TGFβ/BMP Signaling; Bone Microarchitecture.

1. Introduction

Bone homeostasis is a lifelong process in which bone is remodeled by the concerted actions of bone forming osteoblasts and bone resorbing osteoclasts (1). Moreover, osteoblast derived osteocytes are mechanosensors that coordinate the activity of osteoblasts and osteoclasts (1). Osteoblasts also play essential roles in regulating hematopoietic cells in the bone marrow (2). Many signaling pathways are crucial for proper bone development and homeostasis, especially the Transforming Growth Factor β (TGFβ) and Bone Morphogenetic Protein (BMP) signaling pathways (3, 4). Canonical TGFβ/BMP signaling is transduced through downstream effector R-Smads, Smad2/3 (TGFβ) and Smad1/5/8 (BMP). The activation of R-Smads is mediated by a ligand binding induced dimerization of Type I and Type II TGFβ or BMP receptors, resulting in phosphorylation and activation of the R-Smads. Activated R-Smads then bind with Smad4, and translocate to the nucleus to promote transcription of TGFβ/BMP target genes (3, 4). The TGFβ/BMP signaling pathway is evolutionarily conserved in metazoans and plays many crucial roles in bone and cartilage development and homeostasis. TGFβ/BMP dysregulation results in various osteochondrodysplasias and other diseases, including cancer (4).

Jab1, also known as Cops5/Csn5, is an essential component of the evolutionarily conserved COP9 Signalosome (CSN) complex (5). Jab1 is the only CSN subunit that harbors a JAMM (Jab1/MPN/Mov34 metalloenzyme) motif necessary for the enzymatic removal of NEDD8 (deNEDDylation), a small, ubiquitin-like protein, from the Cullin subunit of the Cullin-RING Ligases (CRLs), largest family of E3 ubiquitin ligases (5). The CSN complex is required for animal survival, which is highlighted by the fact that the knockout of any individual CSN subunit in mice so far all result in early embryonic lethality (6, 7). Interestingly, Jab1 was also

independently identified as a co-activator of c-Jun and JunD (8). Outside of the CSN complex, Jab1 also plays a versatile role in regulating the localization, stability, and activity of many transcription factors, including p53, HIF-1α, AP-1 family members, and various Smads (8-13). Thus, Jab1 is essential for regulating many cellular functions, including differentiation, apoptosis, proliferation, DNA damage response, and numerous signal transduction pathways (7). Our lab previously demonstrated that Jab1 is necessary for the successive stages of mouse skeletogenesis during embryogenesis, likely through regulating the TFGβ/BMP signaling pathways in a context-specific manner (14, 15). *Prx1-cre*-mediated deletion of *Jab1* specifically in osteochondral progenitor cells of the limb buds resulted in severely shortened limbs at birth with a drastically disorganized epiphyseal growth plate, impaired osteoblastogenesis, decreased chondrogenesis, and a reduced response to BMP signaling (15). On the other hand, the chondrocyte-specific deletion of *Jab1* using a *Col2a1-cre* driver resulted in severe chondrodysplasia and neonatal lethality, with a severe growth plate defect (14). *Col2a1-cre; Jab1*$^{flox/flox}$ chondrocytes displayed increased apoptosis, impaired cell cycle progression, and increased expression of BMP signaling effectors (14). Thus, Jab1 is necessary for proper skeletal development during mouse embryogenesis, at least in part through its regulation of BMP signaling activity, in a stage-specific manner. However, the specific role of Jab1 in osteoblast progenitor cells and postnatal bone growth was unknown until this study.

Thus, to investigate the role of Jab1 in bone homeostasis, we deleted *Jab1* in osteoblast precursor cells using the *Osx1-GFP::Cre* (hereafter referred to as *Osx-cre*) deleter (16). Interestingly, while the *Osx-cre; Jab1*$^{flox/flox}$ conditional knockout (cKO) mice appeared normal at birth, they then all developed progressive dwarfism. Surprisingly, *Jab1 cKO* mice died with 100% penetrance prior to weaning age. Histological and micro-computed tomography (μCT)

analyses revealed that these mice have significantly decreased postnatal bone growth, a delayed secondary ossification center formation, and severely altered bone microarchitecture. Furthermore, there is impaired osteoblast differentiation and mineralization, concomitant with a reduced response to TGFβ/BMP signaling in *Jab1 cKO* osteoblast precursor cells.

2. Materials and Methods

2.1 Mouse Studies

All animal protocols were approved by the IACUC of Case Western Reserve University. All mice were maintained and housed at Case Western Reserve University's animal facility under standard conditions, as in previous studies (14, 15). The *Jab1*$^{flox/flox}$ mice were obtained from Dr. Ruggero Pardi (17). *Osx1-GFP::Cre* mice (16) and *Gt(ROSA)26Sor*^{tm1Sor} (18) mice were purchased from The Jackson Laboratory (Stock No. 006361 and 003309, respectively).

2.2 Cell Culture

The osteoblast precursor cell line MC3T3-E1 (CRL-2593) and mouse bone marrow stromal cell (mBMSC) (CRL-12424) lines were purchased from ATCC (Manassas, VA, USA) and were cultured according to the manufacturer's instructions. For lentiviral infection, MC3T3-E1 and mBMSCs cells were infected with Mission shRNAs (Sigma-Aldrich, St. Louis, MO, USA) specifically targeting *Jab1* (shRNAs 1, 2, and 3 correspond to TRCN0000304598, TRCN0000311065, and TRCN0000302049, respectively) or a Non-Mammalian shRNA control (SHC002V) at MOI = 3 (MC3T3-E1 cells) or MOI = 5 (mBMSCs cells) per the manufacturer's protocol (19). 48 hours after infections, cells were selected using puromycin at concentrations of 3.5μg/mL or 6μg/mL for MC3T3-E1 and mBMSCs, respectively. The Cignal Finder Reporter Array #CCA-901L-12 (Qiagen) was used to measure signal transduction pathway reporter

activities according to the manufacturer's protocol as previously described (19). Briefly, the control and *Jab1*-knockdown MC3T3-E1 cells were reverse transfected by plating into 96-well plates, and signal pathway reporter activities were measured using the dual luciferase assay kit (Promega, Madison, WI, USA) according to the manufacturer's protocol.

Primary mouse calvarial osteoblasts were isolated from P5 *Jab1*$^{flox/flox}$ mice by serial Collagenase P digestions, and expanded for 48hrs, as previously described (20). Cells were then infected with adenoviruses expressing either Cre Recombinase (Ad-Cre) or Green Fluorescent Protein (Ad- GFP) (Gene Transfer Vector Core) at MOI = 500, and analyzed as previously described (14, 15). Osteoblast differentiation was induced by culturing cells in α-MEM supplemented with 5 mM β-Glycerophosphate and 100μg/mL ascorbic acid for 21 days, as previously described (20).

2.3 Western Blotting

Total proteins were extracted from MC3T3-E1 cells and mBMSCs in RIPA buffer (Thermo Fisher Scientific, Waltham, MA, USA), or from mouse primary calvarial osteoblasts in 5% SDS, and supplemented with Halt Protease and Phosphatase Inhibitor Cocktail (Thermo Fisher Scientific). Subsequent western blotting was performed as previously described (14, 15, 19). The antibodies used in this study are listed in Supplementary Table S1.

2.3 RNA Isolation, cDNA Synthesis, and Real-Time Quantitative RT-PCR

Total RNAs were isolated from MC3T3-E1 cells and primary calvarial osteoblasts using TRIzol reagent (Invitrogen) and the PureLink RNA Mini kit (Ambion, Foster City, CA, USA) as previously described (14, 15, 19). The primers in this study are listed in Supplementary Table S2.

2.4 Histology

The entire P18 mouse hindlimbs were separated from the pelvis, placed into a cassette with the lateral side down, and fixed for 16 hrs in 10% neutral buffered formalin. After 3 washes of PBS, the hindlimbs were decalcified in 0.5M EDTA for 21 days. Tissues were then embedded in paraffin, sectioned at 5µm thickness, and stained with H&E as previously described (14, 15, 19, 21). Von Kossa staining (22), Oil Red O Staining, (23), and β-galactosidase staining (24) was performed as previously described.

2.5 Micro-Computed Tomography (µCT)

Whole tibiae were excised from P18-P20 mice and fixed in 10% neutral buffered formalin for 16 hrs. After 3 washes in PBS, the samples were stored in 70% ethanol at 4°C. Prior to µCT analysis, tibiae were first rehydrated in PBS containing calcium and magnesium to minimize mineral dissolution (25). Scans were conducted in a Bruker SkyScan1172 (Bruker MicroCT, Kontich, Belgium) with a 11 MPix camera at an isotropic voxel size of 8µm employing a 0.5mm thick aluminum filter. An applied x-ray tube voltage of 50kV with an x-ray intensity of 100µA was applied over 180 degrees of rotation with acquisition every 0.45 degrees. Reconstruction was carried out with a modified Feldkamp algorithm (26) using the SkyScan NRecon software accelerated by GPU (27). Tibial reconstruction alignments were adjusted with SkyScan DataView software to a consistent orientation. The selection of the Region/volume of interest (ROI/VOI), the segmentation to binary, and the morphometric analysis were all performed using SkyScan CT-Analyser ("CTAn") software. Morphometry measurements for both cortical and trabecular bone were based on previously reported guidelines (28). Tibial lengths were measured from proximal to distal epiphyses. The cortical VOI was defined as 0.5mm (62 slices) beginning 10 slices proximally offset (0.08mm) from 58% of the metaphysis-metaphysis length, which is the mean position of the tibia-fibula junction (TFJ) in wild type

mice. At this age, the proximal metaphysis does not have a clear cortical-trabecular separation (29). Therefore, the entire proximal metaphysis was analyzed for 3D trabecular morphometry. Due to significant size differences among genotypes, the analysis of trabecular VOI was defined as 25% of the metaphysis-metaphysis length.

2.6 Statistical Analysis

All experiments were conducted using at least 3 biological replicates. Data are expressed as mean ± standard deviation. With the exception of μCT data, all statistical analysis was performed using a 2-tailed Student's t-test on normally distributed data, with $p < 0.05$ considered significant. Statistical tests on μCT data were performed with GraphPad Prism version 8.4.2 software (GraphPad Software, La Jolla, CA, USA). Data were assessed using D'Agostino & Pearson normality testing and Brown-Forsythe test for Equal Variance. Normally distributed data exhibiting equal variance were analyzed by one-way ANOVA with post-hoc analysis by Bonferroni's multiple comparisons test. Data that were not normally distributed or displaying equal variance were tested by Kruskal-Wallis one-way ANOVA with post-hoc analysis by Dunn's multiple comparisons test.

3. Results

3.1. The loss of Jab1 in osteoblast progenitor cells results in a progressive postnatal dwarfism phenotype and early lethality.

To investigate the specific role of Jab1 in postnatal bone growth, we deleted *Jab1* specifically in osteoblast precursor cells with a commonly used *Osx-cre* deleter to generate *Osx-cre; Jab1* $^{flox/flox}$ (*Jab1 cKO*) mice (16). To confirm the cells targeted by the *Osx-cre* transgene, we first crossed *Osx-cre* only mice with *Rosa26-LacZ* mice. The β-galactosidase staining of long

bones from *Osx-cre; Rosa26-LacZ* mice revealed the expression of *Osx-cre* in osteoblasts lining the diaphyseal periosteum, the trabecular bone, the secondary ossification center, and also in the hypertrophic chondrocytes and osteocytes, as previously reported (30, 31) (Figure S1). It was previously reported that the expression of the *Osx-cre* transgene alone might result in a minor bone phenotype in mice (30, 32, 33). Thus, in this study, we performed all mouse experiments using *Osx-cre* only mice as controls, in addition to wild type controls.

Both *Jab1 cKO* and *Osx-cre* only mice appeared grossly normal at birth and through 6 days of age. By 7 days of age, both *Osx-cre* only and *Jab1 cKO* mice begin to develop dwarfism. Our results are in agreement with previous studies showing a decrease in the length and weight of *Osx-cre* only mice at around 1 week of age (30, 33). However, whereas the *Osx-cre* only mice have a normal lifespan/healthspan, and their length stabilizes thereafter, the dwarfism in *Jab1 cKO* mice progressively worsened and they also began to appear lethargic around postnatal day 12 (Figure 1A). Unexpectedly, all *Jab1 cKO* mice die by postnatal day 21, around their weaning age. Indeed, *Jab1 cKO* mice had significantly decreased body length and weight by postnatal day 18 compared with wild type mice and *Osx-cre* only controls (Figure 1B). These results demonstrate that the expression of *Jab1* in osteoblast precursor cells is essential for survival and for maintaining normal postnatal growth in mice.

3.2. The loss of Jab1 in osteoblast precursors drastically alters trabecular and cortical bone structure and delays the formation of the secondary ossification center.

Next, we collected tibiae from 18-21-day old wild type, *Osx-cre* only, and *Jab1 cKO* mice to identify the overall differences in bone structure of early postnatal bones. Histological analysis revealed that the primary trabeculae in *Jab1 cKO* mice are thinner compared with wild

type and *Osx-cre* only mice (Figure 2A). Proper secondary ossification center formation is critical for growth plate formation and long bone growth. Interestingly, our histological analysis also revealed that the secondary ossification center in *Jab1 cKO* mice was much smaller than both the wild type and *Osx-cre* only mice (Figure 2B). This might be due to a delay in the initial formation of the SOC, as the histology at postnatal day 9 shows a drastically decreased size of the secondary ossification center in *Jab1 cKO*, which persists through postnatal day 16 (Figure S2). The histology also uncovered that the cortical bone is more porous in *Jab1 cKO* mice compared with *Osx-cre* only and wild type mice (Figure 2C). Thus, *Jab1* expression in osteoblast precursor cells is critical for proper secondary ossification center formation and proper bone growth.

3.3. Jab1 deficiency in osteoblast precursor cells severely impairs bone microarchitecture.

To further characterize the *in vivo* effect of *Jab1* loss on postnatal bone growth, we performed detailed micro-computed tomography (μCT) analysis on the tibiae of 18-21-day-old wild type, *Osx-cre* only, and *Jab1 cKO* mice. Representative reconstructions of tibiae from each genotype are presented in Figure 3A. First of all, we observed some heterogeneity among individual samples of *Jab1 cKO* tibiae (Figure S3). Nonetheless, in agreement with the length measurements of the entire mouse (Figure 1B), μCT reconstructions and quantification of the tibial length confirmed that *Jab1 cKO* mice had significantly shorter tibiae compared with wild type and *Osx-cre* only mice (Figures 3A and 3B). Next, μCT quantification revealed that both the periosteal and endosteal perimeter were significantly decreased in *Jab1 cKO* mutants, indicating decreased bone size (Figure S4). Moreover, similarly to our histological analysis, the μCT analysis revealed that the primary trabecular bone in *Jab1 cKO* and *Osx-cre* only mice

appeared to be decreased when compared with wild type mice (Figure 3A, third row, and Figure S5A). Indeed, uCT quantification of trabecular bone confirmed that there were significant decreases in the trabecular thickness of *Jab1 cKO* and *Osx-cre* only tibiae compared with wild type tibiae. There was also a trend towards increased trabecular separation in *Jab1 cKO* bones compared with *Osx-cre* only and wild type bones (Figure 4A). Additionally, uCT quantification of trabecular bone volume (BV) and total volume (TV) revealed a significant decrease in *Jab1 cKO* tibiae compared with wild type tibiae, as expected based on the smaller size of *Jab1 cKO* mice (Figures 1A and 4B). We also observed a trend towards decreased BV and TV in the tibiae of *Jab1 cKO* mice when compared with *Osx-cre* only mice (Figure 4B). However, due to the proportional decrease in both bone volume and tissue volume within genotypes, the bone volume fraction (BV/TV) was not significantly changed among *Jab1 cKO, Osx-cre* only, and wild type controls (Figure 4B). Furthermore, uCT analysis demonstrates that the cortical bone was thicker in both *Jab1 cKO* and *Osx-cre* only tibiae compared with wild type (Figures 3A, 5A, and S5B). Furthermore, when compared with wild type tibiae, the cortical bone area (BA) was either slightly decreased in *Jab1 cKO* or was similar in *Osx-cre* only tibiae. There were also decreases in the total cross sectional area (TA) in *Jab1 cKO* and *Osx-cre* only tibiae compared with wild type tibiae. Thus, when compared with wild type, there was a significantly increased cortical bone area fraction (BA/TA) in *Osx- cre* only mice, which was exacerbated in *Jab1 cKO* mice (Figure 5B). Interestingly, cross sections of cortical bone appeared to be more porous in *Jab1 cKO* and *Osx-cre* only bones compared with wild type bones, similarly to our histological analysis (Figures 2C and 3A, bottom row).

Intriguingly, in some *Jab1 cKO* bones, a large portion of their proximal and distal ends appeared to be poorly mineralized (Figure 3C), even though gross examinations showed that

there were tissues present in these areas. We also observed that multiple *Jab1 cKO* mice had callus-like structures present near their distal tibiofibular junction (Figures 3A, 3D, and S3). In contrast, no similar callus-like structures were ever identified in any of the tibiae isolated from wild type or *Osx-cre* only mice (Figure S3). A closer examination of this callus-like structure in *Jab1 cKO* tibiae revealed that the area inside this callus-like structure was likely to be newly formed bone (Figure 3D). This finding suggests that *Jab1 cKO* bones might be more susceptible to incurring spontaneous fractures compared with wild type and *Osx-cre* only bones. Therefore, the loss of *Jab1* in osteoblast precursors significantly alters long bone microarchitecture, impairs proper mineralization, and might lead to spontaneous fractures.

3.4. The loss of Jab1 in osteoblast precursors inhibits osteoblast differentiation and mineralization, likely in part through the positive regulation of TGFβ/BMP signaling.

Our previous study in *Prx1-cre; Jab1*$^{flox/flox}$ mice showed that *Jab1* positively regulates BMP signaling in osteochondral progenitor cells (15). Thus, we hypothesized that the loss of *Jab1* specifically in osteoblast precursor cells also results in impaired BMP-mediated osteoblast differentiation and mineralization. To this end, we first knocked down *Jab1* expression in primary calvarial osteoblasts isolated from *Jab1*$^{flox/flox}$ mice, using adenoviruses expressing either Cre Recombinase (Ad-Cre) or, as a control, a GFP reporter (Ad-GFP) (14, 15). We first confirmed the *Jab1* knockdown efficiency at the RNA and protein levels (Figure 6A). Next, we cultured the primary osteoblasts in osteoblast differentiation media for 21 days and examined mineralization status by performing Von Kossa staining (Figure 6A). Von Kossa staining revealed fewer black nodules in *Jab1*-knockdown versus control primary osteoblasts, indicating that *Jab1* is required for robust osteoblast differentiation and mineralization. To confirm this

finding, we also performed *Jab1*-knockdown experiments in a widely used mouse preosteoblastic cell line, MC3T3-E1 (34), using lentiviral shRNAs specifically targeting *Jab1*. Again, von Kossa staining revealed that the depletion of *Jab1* expression nearly abolished nodule formations in MC3T3-E1 cells as well (Figure 6B). Together, these results confirm that *Jab1* deficiency drastically reduced osteogenic potential in osteoblast precursor cells, which may account for the impaired mineralization and altered bone structure observed in our histological and μCT analyses of *Jab1 cKO* mice (Figures 2 and 3).

Mesenchymal stem cells (MSCs) are multipotent cells with the ability to differentiate into multiple mesenchymal cell lineages, including osteoblasts and adipocytes (35). It is also well-established that the loss of osteogenic differentiation is often associated with an increased adipogenic potential (35). Thus, to determine the effect of *Jab1* loss on MSC adipogenesis, we performed a lentiviral *Jab1*-knockdown in a mouse bone marrow stromal cell (mBMSC) line, and then induced them to differentiate into adipocytes (Figure 6C). Indeed, we found that there were increased lipid droplets in mBMSCs by Oil Red O staining in *Jab1*-knockdown mBMSCs. Thus, the loss of Jab1 might lead to an increase in adipogenic potential and decreased osteoblast differentiation and mineralization.

To further explore the underlying mechanism of *Jab1*-mediated osteoblast differentiation, we next examined the expression of a master osteoblast differentiation transcription factor Runx2 upon *Jab1*-knockdown in osteoblast precursor cells (36). Interestingly, we found that the loss of *Jab1* in MC3T3-E1 cells resulted in no significant change in the Runx2 expression at either the RNA or protein level (Figure 7A and 7B). However, we detected a significant decrease in the mRNA expression of *Osteocalcin*, the most specific late-stage marker of osteoblast differentiation, in *Jab1*-knockdown MC3T3-E1 cells (Figure 7A). This finding is consistent with

the mineralization defect we observed in *Jab1 cKO* mice (Figures 3C), indicating that the loss of *Jab1* in osteoblast precursors might lead to a late-stage differentiation defect. Next, to determine the effect of *Jab1* loss on major signaling pathways, we performed an unbiased reporter screen in MC3T3-E1 cells (Figure 7C). Impressively, we found that of 45 major signaling pathway reporters, 31 (68%) of them were clearly altered in MC3T3-E1 cells upon *Jab1*-knockdown (Figure 7C). Furthermore, of those 31 reporters, 26 (83%) were downregulated, including a Smad2/3 reporter for the TGFβ pathway (Figure 7C). All together, these data are consistent with the established function of *Jab1* as a transcriptional co-factor and with others' previous reports demonstrating a link between Jab1 and the TGFβ/BMP signaling pathway (8, 11, 12, 14, 15, 37-39).

TGFβ is crucial for many aspects of bone biology and osteoblast differentiation, and is tightly regulated at many levels. Therefore, we decided to further investigate the effect of *Jab1* loss on osteoblast's response to TGFβ/BMP stimulation. When primary mouse calvarial osteoblasts were cultured in osteoblast differentiation media for 21 days, *Jab1* was expressed at both an early (Day 0) and a late stage (Day 21) of osteoblast differentiation (Figure 7D), hinting that *Jab1* is required throughout osteoblast differentiation. We also observed a higher level of phospho-Smad1/5/8, a key downstream BMP effector, at Day 21 versus Day 0 (Figure 7D). Next, we infected primary calvarial osteoblasts isolated from $Jab1^{flox/flox}$ mice with adenoviruses expressing either Cre Recombinase (Ad-cre) or a GFP control (Ad-GFP), induced them to differentiate into osteoblasts, and performed western blotting for phospho-Smad1/5/8 (Figure 7E). Interestingly, we found that a decrease in the levels of Jab1 resulted in a major decrease in the levels of phospho-Smad1/5/8 in primary osteoblasts (Figure 7E). Furthermore, we treated control and *Jab1*-knockdown MC3T3-E1 preosteoblasts with BMP7 (300ng/mL) or TGFβ-3

(2ng/mL), and determined the expressions of phospho-Smad1/5/8 and phospho-Smad2/3, a key TGFβ downstream effector, respectively (Figure 7F). Indeed, there was a decreased response to both TGFβ and BMP signaling upon *Jab1*-knockdown in MC3T3-E1 cells. These results suggest that *Jab1* promotes osteoblast differentiation and mineralization at least in part through stimulating TGFβ/BMP signaling.

4. Discussion

Jab1 is an essential subunit of the COP9 Signalosome, and regulates many vital cellular functions, including cell proliferation, differentiation, and apoptosis. Indeed, the conditional knockout of *Jab1* in any given tissue studied to date all results in severe defects to progenitor cell survival and differentiation (5). Our previous work has demonstrated that, as a master developmental regulator, Jab1 is necessary for the successive stages of skeletogenesis by regulating the TGFβ/BMP signaling pathways in a context-specific manner (14, 15). Interestingly, master developmental regulators are often reactivated during tumorigenesis to promote malignancy via their specific effects on cell proliferation, differentiation, and survival. Indeed, as a potential oncogene, *JAB1* has been shown to be overexpressed in many different forms of cancer (7). To that end, we have recently demonstrated that *JAB1* overexpression specifically in osteoblasts can increase the incidence of p53-dependent osteosarcoma formation in mice (19). Moreover, a recently developed small molecular inhibitor of *JAB1*, CSN5i-3, has shown promising results in reducing cell viability, including in osteosarcoma (19). Therefore, a better understanding of the physiological role of Jab1 in osteoblasts will facilitate the development of better Jab1-targeted therapeutic options for osteosaercoma and other cancers.

In the present study, we provide strong evidence that the expression of *Jab1* in osteoblast precursor cells is essential for proper postnatal bone growth and osteoblast differentiation in mice, likely at least in part through the regulation of TGFβ/BMP signaling. To our knowledge, whereas dwarfism and impaired bone structure is relatively common in mice in which a gene of interest is deleted using the the same *Osx-cre* driver, early postnatal lethality is extremely rare among them. Very strikingly, *Jab1 cKO* mutant mice all die around weaning age. While the *Osx-cre* transgene mainly targets cells at the earliest stages of osteoblast differentiation, it is also known to target some other cell types, including hypertrophic chondrocytes, osteocytes, stromal cells, and perivascular cells (30, 31). Indeed, our β-galactosidase staining in *Osx-cre; Rosa26 LacZ* tibiae revealed strong LacZ expressions in osteoblasts, as well as osteocytes and hypertrophic chondrocytes (Figure S1). Because osteoblasts constitute a major component of the hematopoietic stem cell niche (2), we speculate that the early lethality in *Jab1 cKO* mice might result from defective hematopoiesis. Interestingly, a recent study demonstrated that *Osx-cre*-mediated deletion of *Tgfbr2* resulted in early lethality at 4-weeks of age, dwarfism, reduced osteoblast maturation, and perturbed hematopoiesis (40). Additionally, Jab1 has been linked to hematopoietic defects in mice (41, 42). Thus, the early lethality of *Jab1 cKO* mice might be the result of defective hematopoiesis, through the regulation of the HSC niche and/or through TGFβ/BMP signaling, which warrants further investigation.

Osx-cre transgenic mice by themselves were reported to have a transient dwarfism phenotype (30, 33). However, despite our study corroborating the finding that *Osx-cre* only mice are smaller beginning at P7, the *Jab1 cKO* mice were still significantly smaller than *Osx-cre* only mice at postnatal day 18 (Figures 1 and 3A). It is also important to note that the expression of the Osx-cre transgene by itself did not affect osteoblast differentiation (33), thus the bone defects

observed in the *Jab1 cKO* mice were most likely due to the effect of *Jab1* deletion. Indeed, the bone defects observed in some *Jab1 cKO* mice were so severe that the mineralization could not even be detected by μCT, and spontaneous fractures occurred (Figure S3). Thus, based on the early lethality, significantly shorter stature, multiple bone defects, and changes in most μCT parameters, we conclude that *Jab1* plays an essential role in maintaining proper bone microarchitecture in mice.

In contrast to what we previously reported in mice with *Jab1* deleted specifically in chondrocytes, where we found an enhanced response to exogenous BMP treatment (14), the loss of *Jab1* in osteoblast progenitor cells resulted in a reduced response to BMP treatment, highlighting the context-specific role of *Jab1* in the regulation of key developmental signaling pathways. Indeed, *Jab1* has been reported to positively and negatively regulate TGFβ/BMP signaling through controlling the stability and degradation of Smad7 and Smad4, respectively (11, 12). Moreover, several studies have shown that Jab1 inhibits BMP signaling by negatively regulating Smad1/5 (14, 37, 43). As the TGFβ/BMP signaling pathway is tightly regulated at multiple levels (4, 44), the role of *Jab1* in regulating TGFβ/BMP signaling during skeletal development is likely to be highly context-dependent, and remains to be further investigated.

Our reporter assay indicates that *Jab1* activates many signal transduction pathways in osteoblasts. Notably, a canonical Smad2/3 TGFβ reporter activity decreased upon *Jab1* deletion, and the response to exogenous TGFβ/BMP stimulation was also reduced in osteoblasts. Moreover, in both primary calvarial osteoblasts and preosteoblastic MC3T3-E1 cells, the mineralization was greatly reduced upon loss of *Jab1* (Figure 6). Additionally, we provide evidence that the loss of *Jab1* resulted in a shift from osteoblastogenesis to adipogenesis in mouse bone marrow stromal cells. It is well-established that low bone mass can result from a

lineage shift in mesenchymal stem cells from osteoblasts to adipocytes, which can contribute to osteoporosis (45). Thus, a better understanding of the role of *Jab1* in promoting osteoblast differentiation and postnatal bone growth in osteoblast precursor cells might help promote better therapeutic treatments of bone diseases such as osteoporosis.

CRediT Authorship Contribution Statement

W. E. Samsa: Conceptualization, Data curation, Formal analysis, Funding acquisition, Investigation, Methodology, Supervision, Validation, Visualization, Writing – original draft preparation and review and editing

M. K. Mamidi: Formal analysis, Investigation, Methodology, Validation, Writing – review and editing

B. S. Hausman: Data Curation, Formal analysis, Investigation, Methodology, Validation, Visualization, Writing – review and editing

L. A. Bashur: Formal analysis, Funding acquisition, Investigation, Methodology, Validation

E. M. Greenfield: Formal analysis, Methodology, Writing – review and editing

G. Zhou: Conceptualization, Data curation, Formal analysis, Funding acquisition, Investigation, Methodology, Project administration, Resources, Supervision, Validation, Visualization, Writing – original draft preparation and review and editing

Declaration of Competing Interest

The authors declare that there are no potential conflicts of interest.

Acknowledgements

The authors thank Dr. Ruggero Pardi for the generous gift of the *Jab1* conditional allele *Jab1*$^{flox/flox}$ mice. The authors also thank Teresa Pizzuto for her expert histology work. This study was supported in part by the NIAMS of the National Institutes of Health R01 AR068361 to G.Z., the NIDCR of the National Institutes of Health R03 DE019190 and DE019190A1S1 to G.Z., and the NIAMS T32 AR007505 to W.E.S. and L.A.B.

REFERENCES

1. Kenkre JS, Bassett J. The bone remodelling cycle. Ann Clin Biochem. 2018;55(3):308-27.

2. Frisch BJ. The hematopoietic stem cell niche: What's so special about bone? Bone. 2019;119:8-12.

3. Salazar VS, Gamer LW, Rosen V. BMP signalling in skeletal development, disease and repair. Nat Rev Endocrinol. 2016;12(4):203-21.

4. Derynck R, Budi EH. Specificity, versatility, and control of TGF-beta family signaling. Sci Signal. 2019;12(570).

5. Li P, Xie L, Gu Y, Li J, Xie J. Roles of Multifunctional COP9 Signalosome Complex in Cell Fate and Implications for Drug Discovery. J Cell Physiol. 2017;232(6):1246-53.

6. Kato JY, Yoneda-Kato N. Mammalian COP9 signalosome. Genes Cells. 2009;14(11):1209-25.

7. Liu G, Claret FX, Zhou F, Pan Y. Jab1/COPS5 as a Novel Biomarker for Diagnosis, Prognosis, Therapy Prediction and Therapeutic Tools for Human Cancer. Front Pharmacol. 2018;9:135.

8. Claret FX, Hibi M, Dhut S, Toda T, Karin M. A new group of conserved coactivators that increase the specificity of AP-1 transcription factors. Nature. 1996;383(6599):453-7.

9. Oh W, Lee EW, Sung YH, Yang MR, Ghim J, Lee HW, et al. Jab1 induces the cytoplasmic localization and degradation of p53 in coordination with Hdm2. J Biol Chem. 2006;281(25):17457-65.

10. Bae MK, Ahn MY, Jeong JW, Bae MH, Lee YM, Bae SK, et al. Jab1 interacts directly with HIF-1alpha and regulates its stability. J Biol Chem. 2002;277(1):9-12.

11. Wan M, Cao X, Wu Y, Bai S, Wu L, Shi X, et al. Jab1 antagonizes TGF-beta signaling by inducing Smad4 degradation. EMBO Rep. 2002;3(2):171-6.

12. Kim BC, Lee HJ, Park SH, Lee SR, Karpova TS, McNally JG, et al. Jab1/CSN5, a component of the COP9 signalosome, regulates transforming growth factor beta signaling by binding to Smad7 and promoting its degradation. Mol Cell Biol. 2004;24(6):2251-62.

13. Samsa WE, Zhou X, Zhou G. Signaling pathways regulating cartilage growth plate formation and activity. Semin Cell Dev Biol. 2016.

14. Chen D, Bashur LA, Liang B, Panattoni M, Tamai K, Pardi R, et al. The transcriptional co-regulator Jab1 is crucial for chondrocyte differentiation in vivo. J Cell Sci. 2013;126(Pt 1):234-43.

15. Bashur LA, Chen D, Chen Z, Liang B, Pardi R, Murakami S, et al. Loss of jab1 in osteochondral progenitor cells severely impairs embryonic limb development in mice. J Cell Physiol. 2014;229(11):1607-17.

16. Rodda SJ, McMahon AP. Distinct roles for Hedgehog and canonical Wnt signaling in specification, differentiation and maintenance of osteoblast progenitors. Development. 2006;133(16):3231-44.

17. Panattoni M, Sanvito F, Basso V, Doglioni C, Casorati G, Montini E, et al. Targeted inactivation of the COP9 signalosome impairs multiple stages of T cell development. J Exp Med. 2008;205(2):465-77.

18. Soriano P. Generalized lacZ expression with the ROSA26 Cre reporter strain. Nat Genet. 1999;21(1):70-1.

19. Samsa WE, Mamidi MK, Bashur LA, Elliott R, Miron A, Chen Y, et al. The crucial p53-dependent oncogenic role of JAB1 in osteosarcoma in vivo. Oncogene 2020. DOI: 10.1038/s41388-020-1320-6.

20. Zhou G, Zheng Q, Engin F, Munivez E, Chen Y, Sebald E, et al. Dominance of SOX9 function over RUNX2 during skeletogenesis. Proc Natl Acad Sci U S A. 2006;103(50):19004-9.

21. Liang B, Mamidi MK, Samsa WE, Chen Y, Lee B, Zheng Q, et al. Targeted and sustained Sox9 expression in mouse hypertrophic chondrocytes causes severe and spontaneous osteoarthritis by perturbing cartilage homeostasis. Am J Transl Res. 2020;12(3):1056-69.

22. Samsa WE, Vasanji A, Midura RJ, Kondratov RV. Deficiency of circadian clock protein BMAL1 in mice results in a low bone mass phenotype. Bone. 2016;84:194-203.

23. Liang B, Cotter MM, Chen D, Hernandez CJ, Zhou G. Ectopic expression of SOX9 in osteoblasts alters bone mechanical properties. Calcif Tissue Int. 2012;90(2):76-89.

24. Zhou G, Garofalo S, Mukhopadhyay K, Lefebvre V, Smith CN, Eberspaecher H, et al. A 182 bp fragment of the mouse pro alpha 1(II) collagen gene is sufficient to direct chondrocyte expression in transgenic mice. J Cell Sci. 1995;108 (Pt 12):3677-84.

25. Gustafson MB, Martin RB, Gibson V, Storms DH, Stover SM, Gibeling J, et al. Calcium buffering is required to maintain bone stiffness in saline solution. J Biomech. 1996;29(9):1191-4.

26. Feldkamp LA, Davis LC, Kress JW. Practical cone-beam algorithm. Journal of the Optical Society of America A. 1984, https://doi.org/10.1364/josaa.1.000612;1.

27. Yan G, Tian J, Zhu S, Dai Y, Qin C. Fast cone-beam CT image reconstruction using GPU hardware. Journal of X-Ray Science and Technology. 2008;16(4):225-34.

28. Bouxsein ML, Boyd SK, Christiansen BA, Guldberg RE, Jepsen KJ, Muller R. Guidelines for assessment of bone microstructure in rodents using micro-computed tomography. J Bone Miner Res. 2010;25(7):1468-86.

29. Bortel EL, Duda GN, Mundlos S, Willie BM, Fratzl P, Zaslansky P. Long bone maturation is driven by pore closing: A quantitative tomography investigation of structural formation in young C57BL/6 mice. Acta Biomater. 2015;22:92-102.

30. Huang W, Olsen BR. Skeletal defects in Osterix-Cre transgenic mice. Transgenic Res. 2015;24(1):167-72.

31. Chen J, Shi Y, Regan J, Karuppaiah K, Ornitz DM, Long F. Osx-Cre targets multiple cell types besides osteoblast lineage in postnatal mice. PLoS One. 2014;9(1):e85161.

32. Davey RA, Clarke MV, Sastra S, Skinner JP, Chiang C, Anderson PH, et al. Decreased body weight in young Osterix-Cre transgenic mice results in delayed cortical bone expansion and accrual. Transgenic Res. 2012;21(4):885-93.

33. Wang L, Mishina Y, Liu F. Osterix-Cre transgene causes craniofacial bone development defect. Calcif Tissue Int. 2015;96(2):129-37.

34. Sudo H, Kodama HA, Amagai Y, Yamamoto S, Kasai S. In vitro differentiation and calcification in a new clonal osteogenic cell line derived from newborn mouse calvaria. J Cell Biol. 1983;96(1):191-8.

35. Chen Q, Shou P, Zheng C, Jiang M, Cao G, Yang Q, et al. Fate decision of mesenchymal stem cells: adipocytes or osteoblasts? Cell Death Differ. 2016;23(7):1128-39.

36. Komori T. Molecular Mechanism of Runx2-Dependent Bone Development. Mol Cells. 2020;43(2):168-75.

37. Sangadala S, Yoshioka K, Enyo Y, Liu Y, Titus L, Boden SD. Characterization of a unique motif in LIM mineralization protein-1 that interacts with jun activation-domain-binding protein 1. Mol Cell Biochem. 2014;385(1-2):145-57.

38. He F, Lu D, Jiang B, Wang Y, Liu Q, Liu Q, et al. X-linked intellectual disability gene CUL4B targets Jab1/CSN5 for degradation and regulates bone morphogenetic protein signaling. Biochim Biophys Acta. 2013;1832(5):595-605.

39. Li J, Gu Z, Li S, Xiao Z, Sun K. Reverse correlation of Jab1 and Smad4 in PANC-1 cells involved in the pathogenesis of pancreatic cancer. Int J Clin Exp Pathol. 2015;8(8):9279-85.

40. Abou-Ezzi G, Supakorndej T, Zhang J, Anthony B, Krambs J, Celik H, et al. TGF-beta Signaling Plays an Essential Role in the Lineage Specification of Mesenchymal Stem/Progenitor Cells in Fetal Bone Marrow. Stem Cell Reports. 2019;13(1):48-60.

41. Mori M, Yoneda-Kato N, Yoshida A, Kato JY. Stable form of JAB1 enhances proliferation and maintenance of hematopoietic progenitors. J Biol Chem. 2008;283(43):29011-21.

42. Sinha S, Dwivedi TR, Yengkhom R, Bheemsetty VA, Abe T, Kiyonari H, et al. Asrij/OCIAD1 suppresses CSN5-mediated p53 degradation and maintains mouse hematopoietic stem cell quiescence. Blood. 2019;133(22):2385-400.

43. Haag J, Aigner T. Jun activation domain-binding protein 1 binds Smad5 and inhibits bone morphogenetic protein signaling. Arthritis Rheum. 2006;54(12):3878-84.

44. Thielen NGM, van der Kraan PM, van Caam APM. TGFbeta/BMP Signaling Pathway in Cartilage Homeostasis. Cells. 2019;8(9).

45. Abdallah BM, Kassem M. New factors controlling the balance between osteoblastogenesis and adipogenesis. Bone. 2012;50(2):540-5.

Figure Legends

Figure 1. Loss of *Jab1* in osteoblast precursor cells resulted in progressive dwarfism and early lethality. (A) Representative pictures of wild type and *Jab1 cKO* mice at postnatal days 6, 12, and 18, displaying the progressive dwarfism. (B) The quantification of the length and weight of wild type, *Osx-cre* only, and *Jab1 cKO* mice at postnatal day 18. Error bars represent means ± SD. ** $p < 0.01$, *** $p < 0.001$, ***** $p < 0.00005$ when *Osx-cre* only and *Jab1 cKO* are compared with wild type. # $p < 0.05$ when *Jab1 cKO* is compared with *Osx-cre* only. Wild type, n = 12; *Osx-cre* only, n = 8; *Jab1 cKO*, n = 9.

Figure 2. *Jab1 cKO* mice exhibited severely altered bone morphology and delayed secondary ossification center formation. Hematoxylin and Eosin staining in the proximal tibiae of wild type, *Osx-cre* only, and *Jab1 cKO* mice at 18 days of age. (A) Representative images of primary trabeculae. Scale bars, 100µm. (B) Representative images of the secondary ossification centers (SOC). Scale bars, 100µm. (C) Representative images of the cortical bone (CB). Scale bars, 50µ.

Figure 3. *Jab1 cKO* mice exhibited severely altered bone microarchitecture and compromised mineralization. (A) The µCT reconstructions of tibiae from *Jab1 cKO*, wild type, and *Osx-cre* only littermates at 18 days of age. Top row: entire tibiae. White arrow, callus-like

structure. Second row: the bone present in the first 25% of the metaphysis from the proximal tibial growth plate. Third row: cross section taken from box in the second row showing trabecular bone inside the metaphysis. Bottom row: cross sections taken at 58% of the diaphyseal length from the proximal tibial growth plate. (B) The μCT quantification of the whole tibial length. Error bars represent means ± SD. ** $p < 0.01$ when *Osx-cre* only and *Jab1 cKO* are compared with wild type. † $p < 0.001$ when *Jab1 cKO* is compared with *Osx-cre* only. Wild type, n = 12; *Osx-cre* only, n = 8; *Jab1 cKO*, n = 9. (C) The μCT reconstructions of three individual *Jab1 cKO* tibiae showing the apparent lack of mineralization at the proximal and distal ends (white arrows). (D) The μCT reconstruction of the callus-like structure in a *Jab1 cKO* tibia. Left, a rotated view of the *Jab1 cKO* tibia from 3A with the callus-like structure indicated by a white arrow. Right, newly formed bone inside the callus-like structure.

Figure 4. Loss of *Jab1* in osteoblast precursors led to reduced trabecular thickness. (A) The μCT quantification of trabecular thickness, trabecular separation, and trabecular number in wild type, *Osx-cre* only, and *Jab1 cKO* mice. (B) The μCT quantification of bone volume (BV), total volume (TV), and trabecular bone volume fraction (BV/TV) in wild type, *Osx-cre* only, and *Jab1 cKO* mice. Wild type, n = 12; *Osx-cre* only, n = 8; *Jab1 cKO*, n = 9. * $p < 0.05$, ** $p < 0.01$, *** $p < 0.001$ by one-way ANOVA with post-hoc analysis by Bonferroni's multiple comparisons test.

Figure 5. Loss of *Jab1* in osteoblast precursors led to increased cortical thickness and cortical bone fraction. (A) The μCT quantification of cortical thickness. (B) The μCT quantification of cortical bone area (BA), total cross sectional area (TA), and cortical bone fraction (BA/TA). Wild type, n = 12; *Osx-cre* only, n = 8; *Jab1 cKO*, n = 9. For parametric analyses, * $p < 0.05$, ** $p < 0.01$, *** $p < 0.001$ by one-way ANOVA with post-hoc analysis by

Bonferroni's multiple comparisons test. For non-parametric analyses, ### $p < 0.001$ by Kruskal-Wallis one-way ANOVA with post-hoc analysis by Dunn's multiple comparisons test.

Figure 6. *Jab1* deficiency inhibited osteoblast differentiation and mineralization *ex vivo*. (A) Left and middle panels: *Jab1* RNA and protein expression levels in control and *Jab1*-knockdown mouse primary calvarial osteoblasts. Right panel: von Kossa staining in control and *Jab1*-knockdown mouse primary calvarial osteoblasts after 21 days of culture in osteoblast differentiation media. (B) Left and middle panels: *Jab1* RNA and protein expression levels in control and *Jab1*-knockdown MC3T3-E1 cells. Right panel: von Kossa staining in *Jab1*-knockdown MC3T3-E1 cells after 21 days of culture in osteoblast differentiation media. (C) Left and middle panel: *Jab1* RNA and protein expression levels in *Jab1*-knockdown mBMSCs. Right panel: oil red O staining of mBMSCs cultures.

Figure 7. *Jab1*-knockdown inhibited osteoblast differentiation likely in part through the TGFβ/BMP signaling pathways. (A) RNA expression levels of *Runx2* and *Osteocalcin* in *Jab1*-knockdown MC3T3-E1 cells. (B) Protein expression levels of Runx2 and Jab1 in *Jab1*-knockdown MC3T3-E1 cells. (C) An unbiased reporter screen in *Jab1*-knockdown MC3T3-E1 cells. The black arrow indicates a canonical Smad2/3 TGFβ reporter. A detailed list of the pathways in this screen can be found in Supplementary Table 3. (D) Western blot analysis of Jab1 and phospho-Smad1/5/8 in primary calvarial osteoblasts cultured in osteoblast differentiation media for 0 and 21 days, respectively. (E) Western blot analysis of Jab1 and phospho-Smad1/5/8 in control and *Jab1*-knockdown primary calvarial osteoblasts after 21 days of culture in osteoblast differentiation media. (F) Western blot analysis of phospho-Smad1/5/8 (top) and phospho-Smad2/3 (bottom) in control and *Jab1*-knockdown MC3T3-E1 cells treated with 300ng/mL BMP7 or 2ng/mL TGFβ-3 for 1 hour, respectively.

Highlights

1. A novel *Osx-cre; Jab1*$^{flox/flox}$ conditional knockout mouse model exhibits early lethality around weaning age.

2. *Osx-cre; Jab1*$^{flox/flox}$ tibiae display severely impaired bone microarchitecture and mineralization.

3. *Jab1* in osteoblasts promotes osteoblast differentiation, at least in part through TGFβ and BMP signaling.

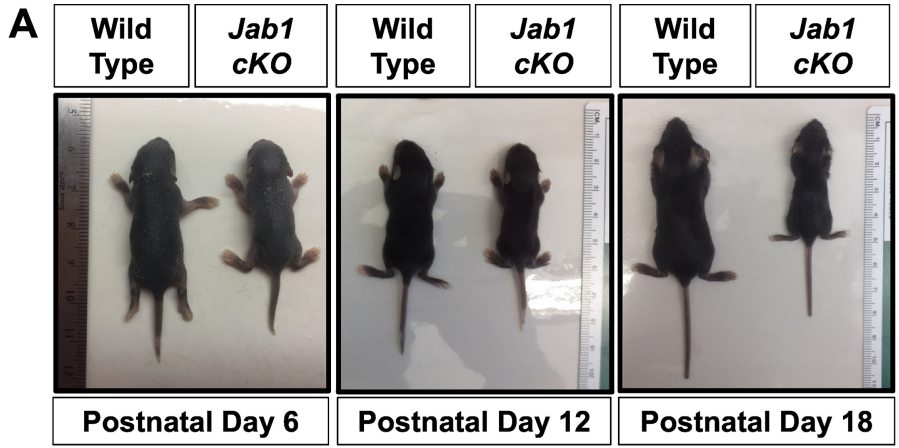
A
Wild Type
Jab1 cKO
Wild Type
Jab1 cKO
Wild Type
Jab1 cKO
Postnatal Day 6
Postnatal Day 12
Postnatal Day 18

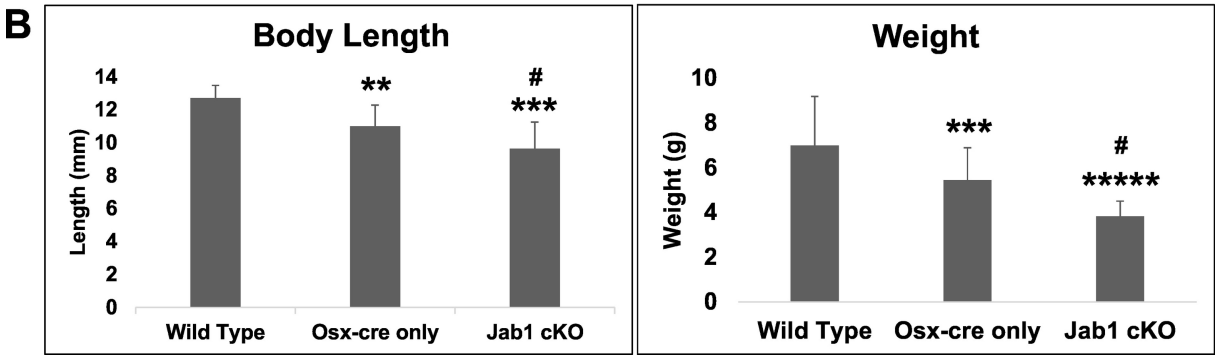
B
Body Length
Length (mm)
14
12
10
8
6
4
2
0
**
#
***
Wild Type
Osx-cre only
Jab1 cKO
Weight
Weight (g)
10
8
6
4
2
0
***
#
*****
Wild Type
Osx-cre only
Jab1 cKO

Figure 1

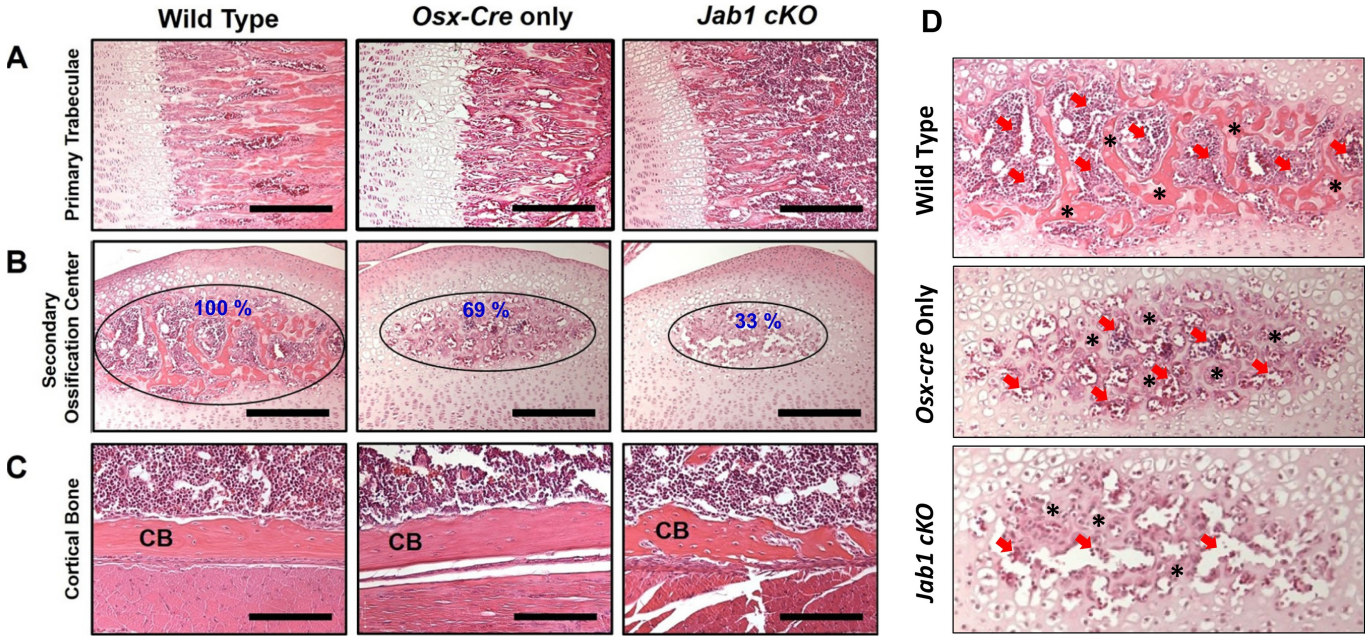
Wild Type
Osx-Cre only
Jab1 cKO
A
Primary Trabeculae
B
Secondary Ossification Center
100 %
69 %
33 %
C
Cortical Bone
CB
CB
CB
D
Wild Type
Osx-cre Only
Jab1 cKO

Figure 2

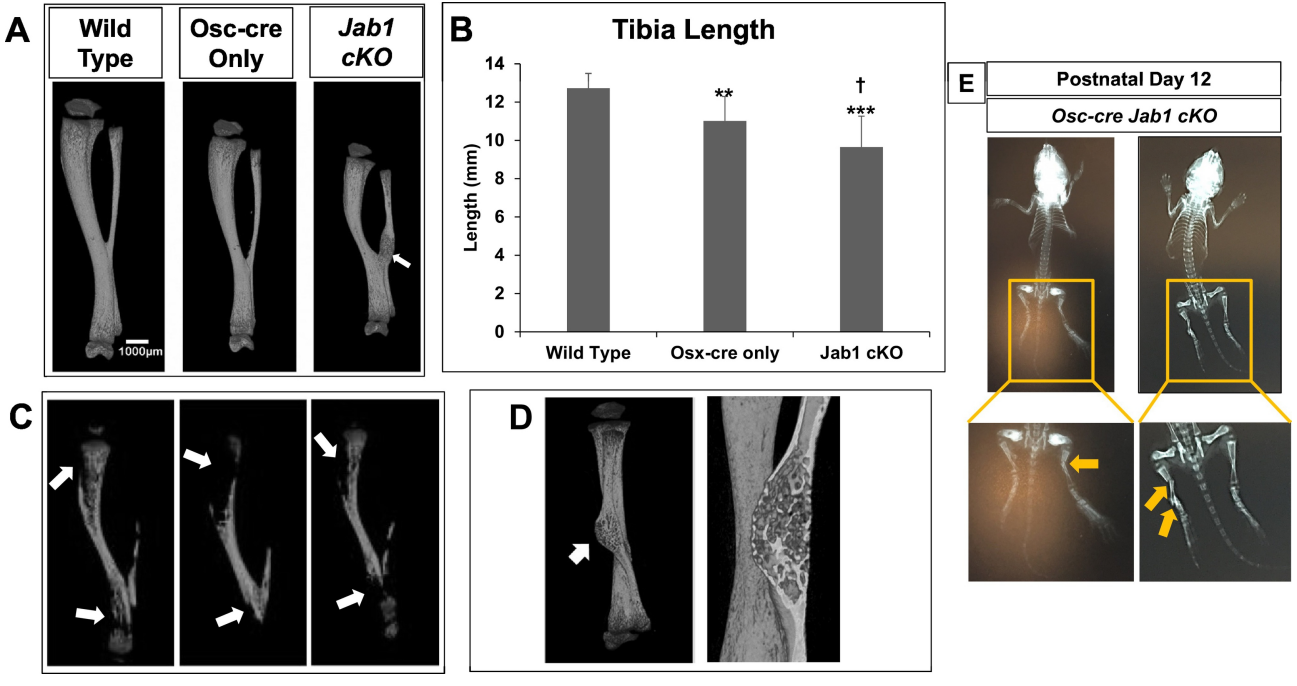
A
Wild Type
Osc-cre Only
Jab1 cKO
1000µm
B
Tibia Length
Length (mm)
14
12
10
8
6
4
2
0
**
†
***
Wild Type
Osx-cre only
Jab1 cKO
C
D
E
Postnatal Day 12
Osc-cre Jab1 cKO

Figure 3

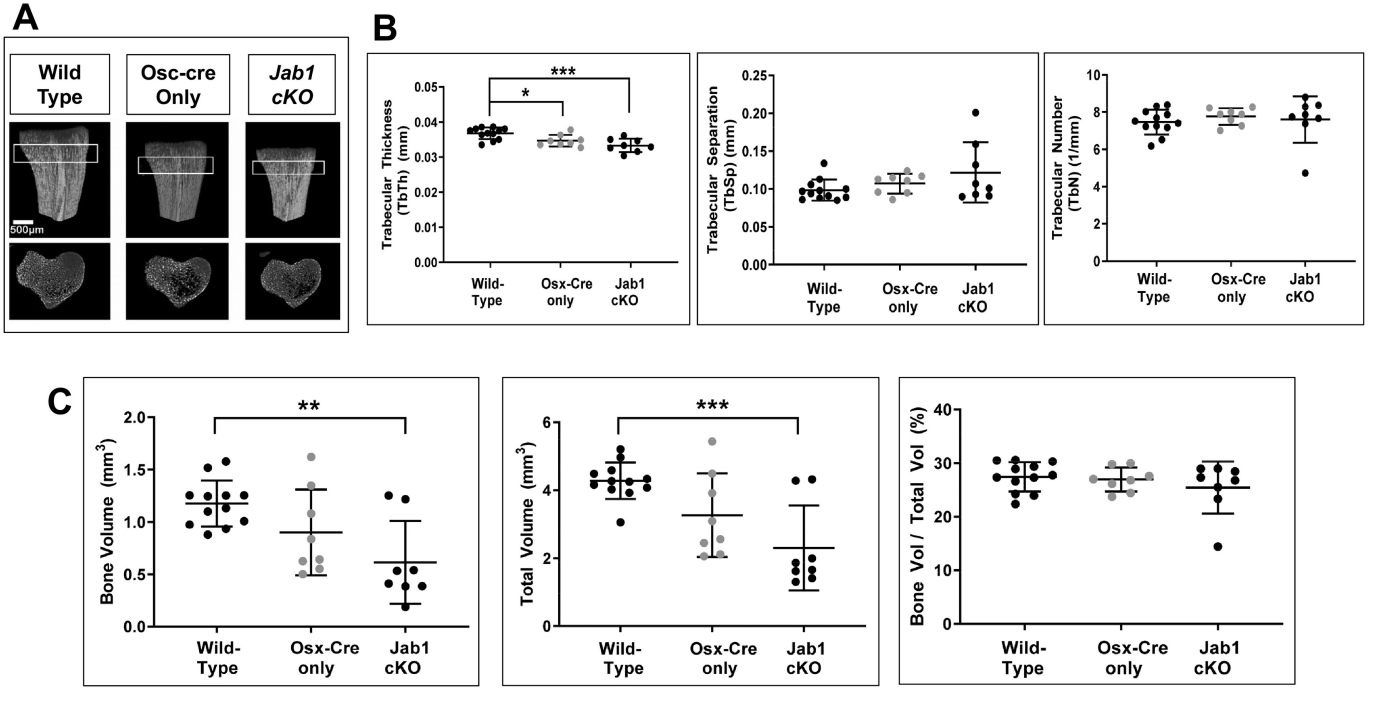
A
Wild Type
Osc-cre Only
Jab1 cKO
500µm
B
Trabecular Thickness (TbTh) (mm)
0.05
0.04
0.03
0.02
0.01
0.00
***
*
Wild-Type
Osx-Cre only
Jab1 cKO
Trabecular Separation (TbSp) (mm)
0.25
0.20
0.15
0.10
0.05
0.00
Wild-Type
Osx-Cre only
Jab1 cKO
Trabecular Number (TbN) (1/mm)
10
8
6
4
2
0
Wild-Type
Osx-Cre only
Jab1 cKO
C
Bone Volume (mm3)
2.0
1.5
1.0
0.5
0.0
**
Wild-Type
Osx-Cre only
Jab1 cKO
Total Volume (mm3)
6
4
2
0
***
Wild-Type
Osx-Cre only
Jab1 cKO
Bone Vol / Total Vol (%)
40
30
20
10
0
Wild-Type
Osx-Cre only
Jab1 cKO

Figure 4

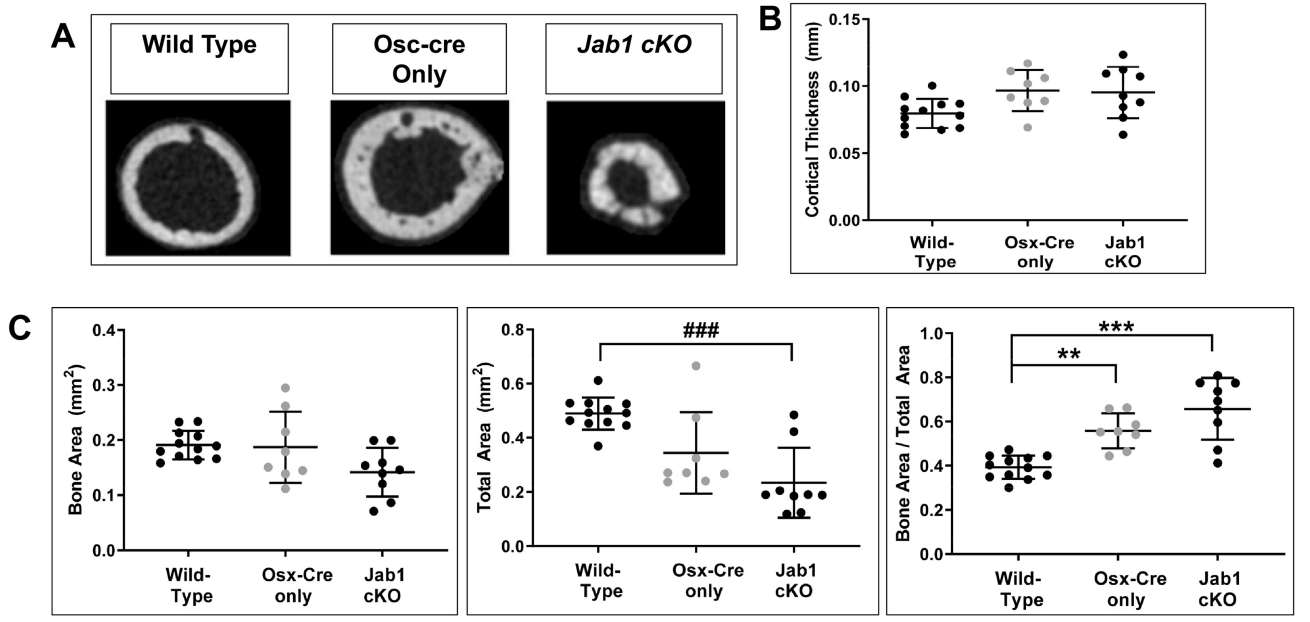
A
Wild Type
Osc-cre Only
Jab1 cKO
B
Cortical Thickness (mm)
0.15
0.10
0.05
0.00
Wild-Type
Osx-Cre only
Jab1 cKO
C
Bone Area (mm2)
0.4
0.3
0.2
0.1
0.0
Wild-Type
Osx-Cre only
Jab1 cKO
Total Area (mm2)
0.8
0.6
0.4
0.2
0.0
###
Wild-Type
Osx-Cre only
Jab1 cKO
Bone Area / Total Area
1.0
0.8
0.6
0.4
0.2
0.0
***
**
Wild-Type
Osx-Cre only
Jab1 cKO

Figure 5

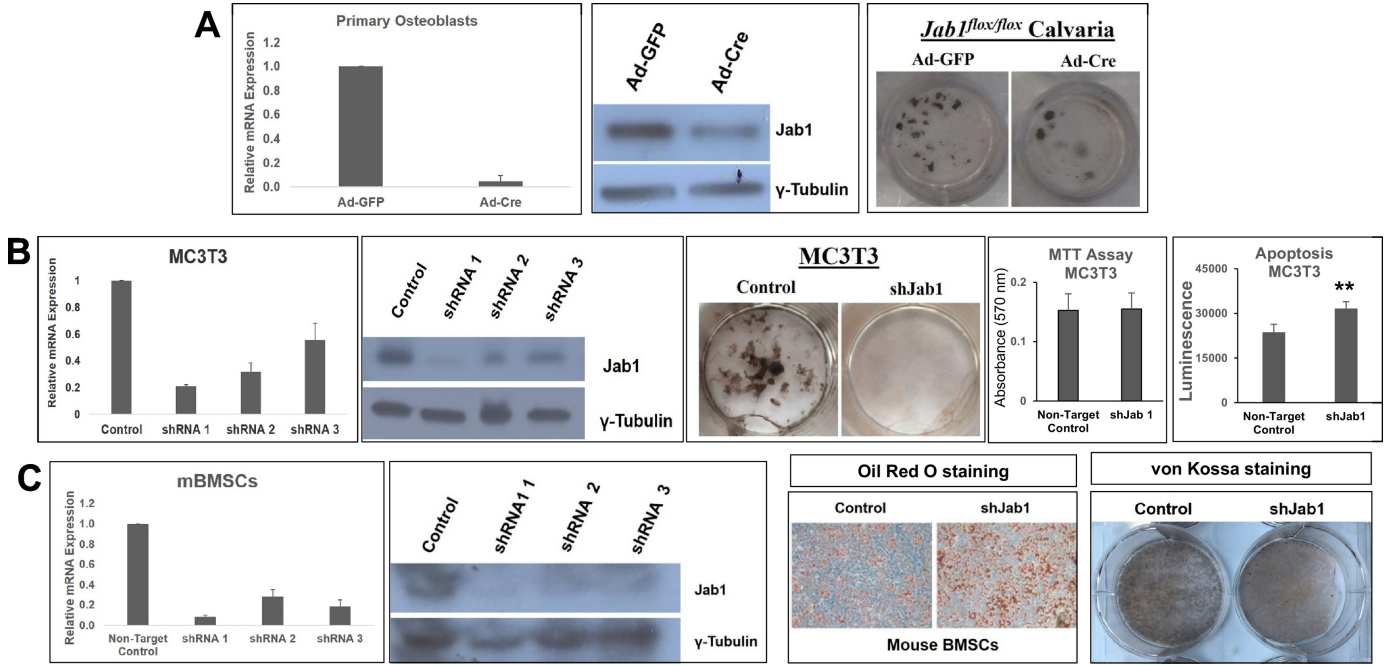
A
Primary Osteoblasts
Relative mRNA Expression
1.2
1.0
0.8
0.6
0.4
0.2
0.0
Ad-GFP
Ad-Cre
Ad-GFP
Ad-Cre
Jab1
γ-Tubulin
Jab1flox/flox Calvaria
Ad-GFP
Ad-Cre
B
MC3T3
Relative mRNA Expression
1
0.8
0.6
0.4
0.2
0
Control
shRNA 1
shRNA 2
shRNA 3
Control
shRNA 1
shRNA 2
shRNA 3
Jab1
γ-Tubulin
MC3T3
Control
shJab1
MTT Assay
MC3T3
Absorbance (570 nm)
0.2
0.1
0
Non-Target Control
shJab 1
Apoptosis
MC3T3
Luminescence
45000
30000
15000
0
**
Non-Target Control
shJab1
C
mBMSCs
Relative mRNA Expression
1.2
1.0
0.8
0.6
0.4
0.2
0.0
Non-Target Control
shRNA 1
shRNA 2
shRNA 3
Control
shRNA 1
shRNA 2
shRNA 3
Jab1
γ-Tubulin
Oil Red O staining
Control
shJab1
Mouse BMSCs
von Kossa staining
Control
shJab1

Figure 6

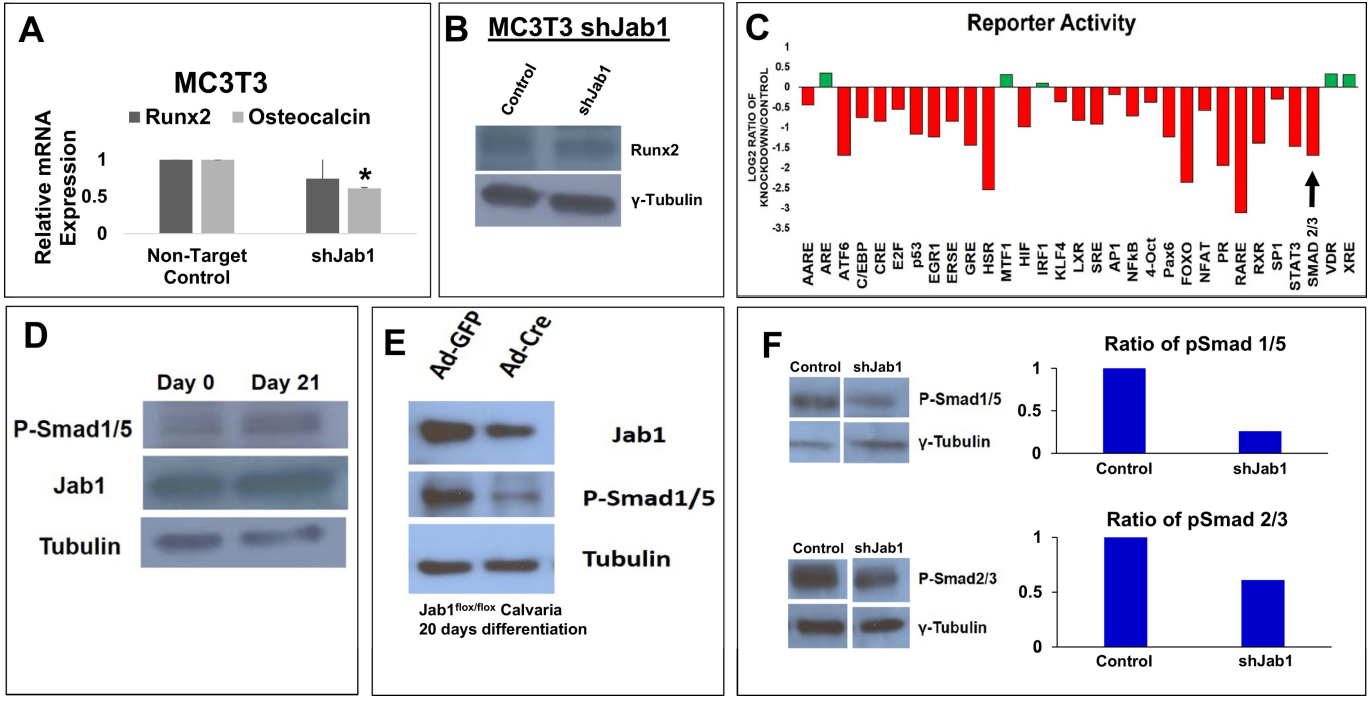
A
MC3T3
Runx2
Osteocalcin
Relative mRNA Expression
1
0.5
0
*
Non-Target Control
shJab1
B
MC3T3 shJab1
Control
shJab1
Runx2
γ-Tubulin
C
Reporter Activity
LOG2 RATIO OF KNOCKDOWN/CONTROL
1
0.5
0
-0.5
-1
-1.5
-2
-2.5
-3
-3.5
AARE
ARE
ATF6
C/EBP
CRE
E2F
p53
EGR1
ERSE
GRE
HSR
MTF1
HIF
IRF1
KLF4
LXR
SRE
AP1
NFkB
4-Oct
Pax6
FOXO
NFAT
PR
RARE
RXR
SP1
STAT3
SMAD 2/3
VDR
XRE
D
Day 0
Day 21
P-Smad1/5
Jab1
Tubulin
E
Ad-GFP
Ad-Cre
Jab1
P-Smad1/5
Tubulin
Jab1flox/flox Calvaria
20 days differentiation
F
Control
shJab1
P-Smad1/5
γ-Tubulin
Ratio of pSmad 1/5
1
0.5
0
Control
shJab1
Control
shJab1
P-Smad2/3
γ-Tubulin
Ratio of pSmad 2/3
1
0.5
0
Control
shJab1

Figure 7